GEOPHYSICAL RESEARCH LETTERS, VOL. 16, NO. 9, PAGES 995-998, SEPTEMBER 1989

OCEANIC HEAT FLUX IN THE FRAM STRAIT MEASURED BY A DRIFTING BUOY

Donald K. Perovich and Walter B. Tucker III

United States Army Cold Regions Research and Engineering Laboratory

Richard A. Krishfield

Woods Hole Oceanographic Institute

Abstract. As one component of the Arctic Environmental Drifting Buoy, two thermistor strings were installed through the ice to measure ice temperatures and determine oceanic heat fluxes as the buoy drifted from the Arctic basin into the Greenland Sea. Ice temperature data between 14 Dec 1987 and 2 Jan 1988 were retrieved. During this period the AEDB progressed from approximately 81°N 4°E to 77°N 5°W. This constituted the most rapid displacement of the entire drift, coinciding with the entry of the floe into the marginal ice zone of Fram Strait. Once in the MIZ, water temperatures increased, most notably at a depth of 16 m, where values changed from –1.8°C to more than 2°C. Bottom ablation rates of 34 mm/day were observed between 21 and 28 Dec. During this excursion into warmer water, the oceanic heat flux increased by a factor of 18, from 7 W/m^2 to 128 W/m^2.

Introduction

Both the extent and the thickness of the polar sea ice covers are sensitive to the transfer of heat from the ocean to the underside of the ice. Maykut and Untersteiner [1971] demonstrated that an oceanic heat flux (F_w) of 2 W/m^2 was consistent with observations of ice equilibrium thickness in the Arctic basin and that an increase to 8 W/m^2 would be sufficient to remove the entire ice cover. Maykut [1982] discussed in detail the impact of the oceanic heat flux on large-scale heat exchange in the Central Arctic. In the Antarctic, Allison [1981], studying sea ice near Mawson, estimated the oceanic heat flux to be in the 10-20 W/m^2 range, while Gordon et al. [1984] report a mean annual F_w of 12 W/m^2 for the Weddell Sea. These large values suggest that the oceanic heat flux may play an even more important role in the annual cycle of Antarctic sea ice.

Direct measurements of sensible heat flux in the ocean are quite difficult and are rife with uncertainties. However, an ice cover provides an opportune platform to monitor indirectly the time-integrated oceanic heat flux. The complex task of measuring detailed temperature and salinity profiles in the water and estimating exchange coefficients is replaced by the considerably simpler job of measuring ice temperature, salinity, and mass changes at the ice bottom. The oceanic heat flux is then computed as the residual of the energy balance equation of the lower portion of the ice. This indirect method has been used successfully by McPhee and Untersteiner [1982], who observed values of F_w less than 1 W/m^2 in the Arctic northwest of Spitzbergen. In sharp contrast to the small Central Arctic values of 1–2 W/m^2, observations in the marginal ice zone of the Greenland Sea during summer indicate oceanic heat fluxes of 1600 W/m^2 at the the extreme ice edge [Josberger, 1987] and 200 W/m^2 roughly 30 km in from the ice edge [McPhee et al., 1987]

Because of the importance of the oceanic heat flux to sea ice thermodynamics and the potential for large spatial variations, values from diverse regions should be obtained. One approach is to acquire these data through buoy-based measurements. In this paper we present data from one such experiment.

Experimental Configuration

The Arctic Environmental Drifting Buoy [Honjo, 1988] was a sophisticated instrument package consisting of ice thermistor strings, Argos transmitters, fluorometers, an acoustic Doppler current profiler, and a sediment trap. On 4 Aug 1987 the buoy was deployed on a multiyear ice floe at 86°17'N, 22°13'E. It drifted on the ice until 2 Jan 1988 (77°36'N, 5°12'W) when the floe broke up while traversing Fram Strait. It floated in the water from 2 Jan until recovery on 15 Apr 1988. In total the buoy drifted nearly 4000 km in 255 days.

The ice temperature portion of the AEDB consisted of two thermistor strings in the ice plus a datalogger in the buoy . The strings were installed adjacent to the buoy in multiyear ice that was 3.7 m thick with a 0.08 m snowcover. One string was a finely spaced (0.05 m) vertical array centered on the bottom of the ice, with more coarsely spaced (0.10, 0.25, 1.00 m) thermistors extending 0.75 m up into the ice and 1.8 m down into the water column. The other string comprised 13 thermistors spaced at 0.25-m intervals from the surface of the ice to a depth of 3.0 m. Prior to installation the thermistors were calibrated in the laboratory at three temperatures to provide an accuracy of 0.01°C. Every 6 hours the datalogger interrogated the thermistor strings and recorded the results.

The ice temperature measurements were terminated on 2 Jan when the ice floe was crushed and the thermistor strings were sheared off from the buoy. Unfortunately, due to a malfunction in the datalogger's storage module, data from the earlier portion of the drift was lost. Because of these two difficulties, the only ice temperature data retrieved were from 14 Dec (day 348) to 2 Jan (day 367). Although only 20 days in duration, this period proved to be most intriguing, manifesting large values of ice speed, bottom melt rate, and oceanic heat flux.

Paper number 89GL01278.

Results

From 14 Dec to 2 Jan the AEDB progressed from roughly 81°N 4°E to 77°N 5°W, which constituted the most rapid displacement of the entire drift. Figure 1 displays the drift track of the buoy during this period. Ice edge positions obtained from the Naval Polar Oceanography Center weekly ice analyses are also shown in Figure 1. There was a sharp increase in displacement on day 357 as the buoy entered the marginal ice zone of the Fram Strait. Between days 357 and 367, the position of the ice floe varied from within 30 to 100 km of the ice edge.

Buoy speed as a function of time is plotted in Figure 2. Speeds from day 348 to 356 are comparable to mean values for the entire experiment. After day 356 the speed increased sharply, with the buoy moving as fast as 80 km/day. The sharp increase in speed as ice enters Fram Strait from the Arctic basin has been pointed out by Moritz and Colony [1988], who examined the drift statistics of many buoys in this region.

Temperatures at selected depths within the ice and the water column are also plotted in Figure 2. The 16-m temperatures were obtained from an RD Instruments acoustic Doppler current profiler (Plueddeman, personal communication, 1989). The ADCP uses a YSI thermolinear component that has an accuracy better than 0.1°C. The 16.0, 5.6, and 3.0 m thermistors were in the water, while the 2.75, 2.50, and 2.25 m probes were initially in the ice. From day 348 to 355 the water column to a depth of 16 m was essentially isothermal at its freezing point. On day 355, associated with the increase in speed, a transition to warmer water occurred. The warmest water temperature (2.25°C) was observed at a depth of 16 m near the end of day 356.

Thermistor data indicate that from day 348 to day 355 the temperature profile in the ice was linear with a gradient of approximately 5°C m^{-1}. Using this linear profile it was straightforward to determine that the ice temperature was equal to the water temperature at a depth of 2.98 m, thereby delineating the bottom of the ice. At any depth, temporal variations in temperature were small—on the order of a few tenths of a degree per day. There was no appreciable bottom ablation during this period. After the floe entered warmer water on day 356 there was a continual increase in temperature in the bottom meter of the ice. This trend was most pronounced for the 2.75 m probe, which melted free of the ice on day 362. Between days 355.25 and 362.00, the ice bottom moved from 2.98 to 2.75 m, constituting 0.23 m of ablation. While large, this average ablation rate of 34 mm/day is comparable to those reported by Maykut and Perovich [1985], Morison et al. [1987], and Josberger [1987] for the summer MIZ. Our measurements occurred in winter, and that even as the underside of the ice was undergoing this considerable ablation, air temperatures ranged from –15 to –30°C.

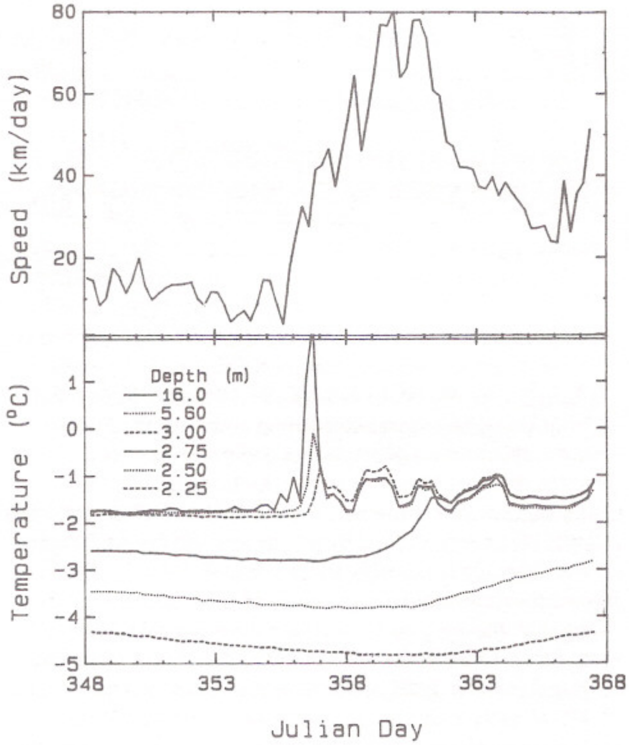

Fig. 2. a) Speed vs time and b) temperature at selected depths vs time. The 16.0, 5.6, and 3.0 m depths were in the water and the 2.75, 2.50, and 2.25 m depths were in the ice. Depths are measured from the surface of the ice.

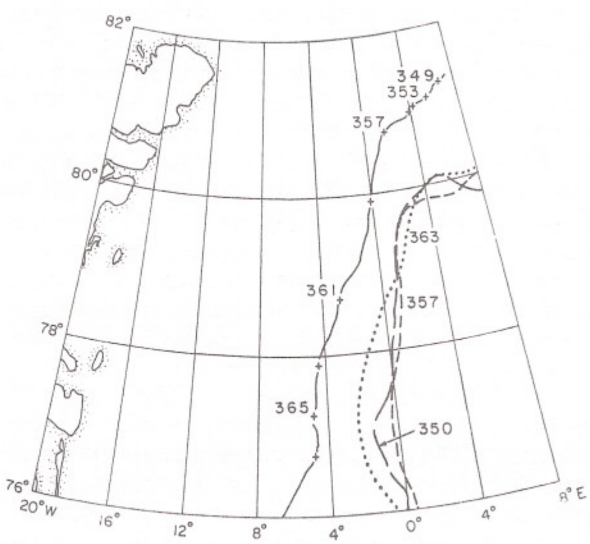

Fig. 1. Map of the AEDB track for days 348 to 367. Ice edge positions are plotted for days 350 (– –), 357 (---), and 363 (···).

McPhee and Untersteiner [1982] describe the method for computing the oceanic heat flux from ice temperature profiles and measurements of ablation/accretion at the ice bottom. The time-averaged oceanic heat flux is the residual of the conductive (Q_f), specific (Q_s), and latent (Q_L) heats,

$$F_w = (1/\Delta t)(Q_f + Q_s + Q_L), \qquad (1)$$

where Q represents heat fluxes integrated over time (t). The latent heat associated with ice formation is negative, and with ice ablation, positive.

The conductive heat term describes the heat flow though a reference level within the ice and is expressed as

$$Q_f = \int k_s(\partial T/\partial z)dt, \qquad (2)$$

where the thermal conductivity of sea ice (k_s) is defined using Untersteiner's [1961] expression

$$k_s = k_i + (\beta s_i / T)$$

k_i is the thermal conductivity of fresh ice (2.04 J m^{-1}), B is a constant equal to 117.3 J m^{-1}s^{-1}, s_i is ice salinity (mass of solute per mass of solution), T is ice temperature (°C), and z is depth.

The specific heat contribution refers to the change in heat content of the ice and is

$$Q_s = \rho \iint c_s dT dz, \tag{3}$$

where ρ is the ice density and c_s is the specific heat of sea ice. Schwerdtfeger [1963] gives the specific heat of sea ice as

$$c_s = -s_i L/(\alpha T^2) + s_i(c_w - c_i)/(\alpha T) + c_i,$$

where α is a constant (–0.0182°C^{-1}), L is the latent heat of fusion for pure ice (333.9 kJ/kg), and the specific heat of pure water (c_w) and pure ice (c_i) are 4.23 and 2.01 kJ°C^{-1}kg^{-1}, respectively. The integration over z is performed from the reference level in the ice to the bottom of the ice.

The latent heat expression is

$$Q_L = \rho \int q_m dz, \tag{4}$$

where q_m is the heat needed to melt a parcel of ice starting from temperature T_o and is given by Schwerdtfeger [1963] as

$$q_m = (L - c_i T_o)[1 - s_i/(\alpha T_o)] + (1/A) s_i (c_w - c_i) \ln(s_i/(\alpha T_o))$$

Equation 1 was evaluated by substituting the expressions for Q_f, Q_s, and Q_L from equations 2, 3, and 4. An ice salinity of 3 ‰ was selected as representative of the lower portion of multiyear ice [Weeks and Ackley, 1982]. The conductive term was calculated using a selected depth of 2 m as a reference level with $\partial T/\partial z$ evaluated using a central difference scheme. The time integral in equation 2 was evaluated numerically using a trapezoid rule with a 6-hr time step. In equation 3 the integration over temperature was performed analytically, while the integration over depth was done numerically using a 0.05-cm spacing. Similarly, the depth integral in equation 4 was computed using the trapezoid rule with a spacing of 0.01 m.

Computations of oceanic heat flux for two time intervals are presented in Table 1. Determining the position of the ice bottom is the largest source of error in the calculations, resulting in an uncertainty of 2 W/m^2. The first interval (days 348.25 to 355.25) is the period prior to the floe entering warmer water. During this period, water temperatures were at or near the freezing point and there was no discernible bottom melting. The second interval (355.25 to 362.00) begins with the entry into warmer water and ends when the 2.75-m thermistor melted free. Heat flux calculations were not performed for days 362 to 367 because the amount of bottom melting could not be accurately determined. As the ice entered warmer water, F_w changed by a factor of 18, increasing from 7 W/m^2 to 128 W/m^2. As Table 1 indicates, virtually all the additional heat was applied to melting on the underside of the ice. This large ocean-ice transfer of sensible heat in the MIZ is not surprising in light of the warm water and the rapid ice movement.

TABLE 1. Summary of heat data for periods from 14 to 21 Dec and from 21 to 28 Dec. Q is the heat per unit area (MJ/m^2), % is the percent of the net Q, and F is the flux (W/m^2).

	348.25 to 355.25			355.25 to 362.00		
	Q	%	F	Q	%	F
Conduction	5.7	134	9.3	5.4	7	9.2
Specific heat	–1.4	–34	–2.4	1.4	2	2.5
Latent heat	0.0	0	0.0	68.0	91	116.6
Ocean	4.2	100	7.0	84.4	100	128.3

Let us now speculate about the earlier portion of the drift. While there are no ice temperature data available from the beginning of the drift on 4 Aug (day 216) through 14 Dec (day 348), we do know that the ice thinned from 3.70 to 2.98 during this period. Two simple scenarios to account for this ice loss are 1) that it occurred in a few discrete warm-water events or 2) that the ice was ablating continuously throughout the drift. Water temperatures at 16 m from day 216 to 367 are shown in Figure 3 (Plueddeman, personal communication, 1989). The excursion into warm water on day 356 is by far the largest thermal event of the drift. Aside from a slight increase in water temperature near day 325, no other such events are apparent. This argues that, at least in a general sense, the mass loss at the bottom was constant during the entire drift.

Constant ice loss would yield an average melt rate of 5.5 mm per day. Assume, somewhat simplistically, that on 4 Aug the ice temperature profile was isothermal (–1.0°C) from 2 to 3.4 m, then decreased linearly to –1.5°C at 3.7 m. Given this initial temperature profile there would have been a latent heat loss of 185 MJ/m^2 due to melting and a change in heat content of –27 MJ/m^2 due to cooling. The conductive heat flux is more difficult to estimate. Untersteiner [1961] indicates that temperature gradients in the ice interior are less than half a degree per meter from August through October, then increase gradually to maximum values in early January. We shall assume that at a depth of 2 m the ice is isothermal from August

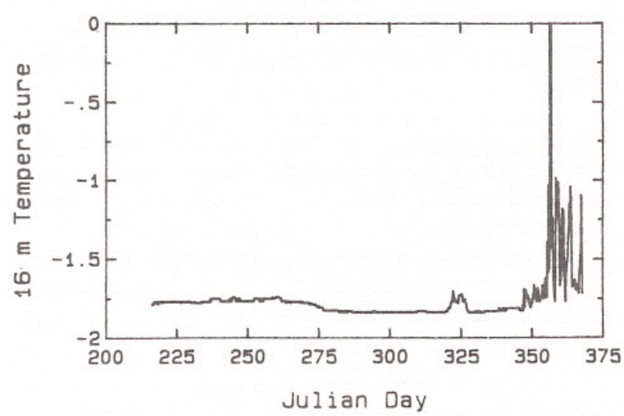

Fig. 3. Water temperature 16 m below the ice surface vs time from 4 Aug 1987 to 2 Jan 1988.

through October, followed by a uniform cooling to the profile observed on 14 Dec, resulting in a conductive heat loss of 7 MJ/m^2. Combining these estimated heats in equation 1,

$$F_w = (7-27+185)/(348-216) = 1.2\ MJ/m^2 day = 14\ W/m^2$$

produces an oceanic heat flux of 14 W/m^2.

Being an order of magnitude larger than standard estimates of oceanic heat flux in the Central Arctic, our time-averaged value is large enough to engender some further discussion. Certainly with the many assumptions there is considerable potential for error. In fact it is suspicious that the estimated flux of 14 W/m^2 is twice as large as the value for the period 348–355. It is evident though that the time-averaged oceanic heat flux will be on the order of 10 W/m^2, rather than 1 W/m^2. However, it is possible that a disproportionate share of the melting occurred in the August–September time frame. During this period the water column is stratified from the input of fresh meltwater so that temperatures at 16 m may not be representative of water temperatures at the ice bottom. In addition there is a sizable input of shortwave radiation into the water column, which could result in enhanced bottom ablation.

Summary

There was 0.72 m of bottom melting between the deployment of the AEDB on 4 Aug 1987 at 86°N 22°E and when it entered Fram Strait on 14 December 1987 at 81°N 4°E. Examination of the 16-m ocean temperature leads us to believe that there were no dramatic melting events during this period. By making some simple assumptions regarding the temperature profile in the ice, we determined that the time-averaged oceanic heat flux was 14 W/m^2. Between 14 Dec and 2 Jan we obtained high-resolution temperature data in the ice and upper ocean. The buoy drifted from 81°N 4°E to 77°N 5°W during this time, reaching speeds as great as 80 km/day. At the onset of the high drift rates, warmer water was encountered, resulting in 0.23 m of bottom ablation over a 7-day winter period. During this period of rapid bottom melting the oceanic heat flux was 128 W/m^2.

Although this experiment was hampered by equipment difficulties, buoy-based systems show promise as an effective means of measuring oceanic heat flux in ice-covered waters. Buoys afford a platform for far-ranging spatial and long-term temporal measurements of F_w. Increased accuracy in F_w could be obtained by reducing uncertainties in ice bottom mass changes through the addition of an independent ice ablation sensor.

Acknowledgments. Thanks to Dr. A.J. Plueddeman for graciously providing the 16-m temperature data. We appreciate the helpful discussion with J. Wettlaufer. This article benefited from the reviews provided by Dr. E.L. Andreas and S.F. Ackley. Finally, we express our gratitude to Dr. S. Honjo for the opportunity to participate in the AEDB effort. This work was funded under ONR Contracts N0001489AF00001 and N0001487K0007.

References

Allison, I., Antarctic sea ice growth and oceanic heat flux, in *Sea Level, Ice and Climate Change*, IAHS Publ. No. 131, 161–170, 1981.

Gordon, A.L., C.T.A. Chen, and W.G. Metcalf, Winter mixed layer entrainment of Weddell Deep water, *J. Geophys. Res., 89*, 637–640, 1984.

Honjo, S., AEDB: Ice-, water-surface drifting buoy mooring experiment through the southern transpolar drift, *EOS Trans. AGU, 69*, 1277, 1988.

Josberger, E.G., Bottom ablation and heat transfer coefficients from the 1983 Marginal Ice Zone Experiments, *J. Geophys. Res., 92*, 7012–7016, 1987.

Maykut, G.A., Large-scale heat exchange and ice production in the central Arctic, *J. Geophys. Res., 87*, 7971–7985, 1982.

Maykut, G.A. and D.K. Perovich, MIZEX heat and mass balance data, *Rep. APL-UW 12-85*, 73 pp. Appl. Phys. Lab., Univ. of Wash., Seattle, 1985.

Maykut, G.A. and N. Untersteiner, Some results from a time dependent, thermodynamic model of sea ice, *J. Geophys. Res., 76*, 1550–1575, 1971.

McPhee, M.G. and N. Untersteiner, Using sea ice to measure vertical heat flux in the ocean, *J. Geophys. Res., 87*, 2071–2074, 1982.

McPhee, M.G., G.A. Maykut, and J.A. Morison, Dynamics and thermodynamics of the ice/upper ocean system in the Marginal Ice Zone of the Greenland Sea, *J. Geophys. Res., 92*, 7017–7031, 1987.

Morison, J.A., M.G. McPhee, and G.A. Maykut, Boundary layer, upper ocean, and ice observations in the Greenland Sea Marginal Ice Zone, *J. Geophys. Res., 92*, 6987–7011, 1987.

Moritz, R.E. and R. Colony, Statistics of sea ice motion, Fram Strait to North Pole, in *Proc. of 7th Intl. Conf. on Offshore Mech. and Arctic Eng., vol 4*, 75–82, 1988.

Schwerdtfeger, P., The thermal properties of sea ice, *J. Glaciol., 4*, 789–807, 1963.

Untersteiner, N., On the mass and heat budget of Arctic sea ice, *Arch. Meteorol. Geophys. Bioklim., Ser. A, 12*, 151–182, 1961.

Weeks, W.F. and S.F. Ackley, The growth, structure, and properties of sea ice, *CRREL Monograph 82-1*, 130 pp, Cold Reg. Res. and Eng. Lab., Hanover, N.H., 1982.

D. Perovich and W. Tucker III, U.S. Army Cold Regions Research and Engineering Laboratory, 72 Lyme Road, Hanover, NH 03755.

R. Krishfield, Woods Hole Oceanographic Institute, Woods Hole, MA 02543.

(Received March 9, 1989;
accepted June 20, 1989)